Soil Ecol. Lett. 2022, 4(1): 78–91
https://doi.org/10.1007/s42832-020-0066-y

RESEARCH ARTICLE

Legacy effect of elevated CO_2 and N fertilization on mineralization and retention of rice (*Oryza sativa* L.) rhizodeposit-C in paddy soil aggregates

Yuhong Li[1], Hongzhao Yuan[1,*], Anlei Chen[1], Mouliang Xiao[1], Yangwu Deng[2], Rongzhong Ye[3], Zhenke Zhu[1], Kazuyuki Inubushi[4], Jinshui Wu[1,5], Tida Ge[1]

1 Key Laboratory of Agro-ecological Processes in Subtropical Region & Changsha Research Station for Agricultural and Environmental Monitoring, Institute of Subtropical Agriculture, Chinese Academy of Sciences, Changsha 410125, China
2 School of Resources and Environmental Engineering, Jiangxi University of Science and Technology, Ganzhou 341000, China
3 Department of Plant & Environmental Sciences, Pee Dee Research & Education Center, Clemson University, Florence, SC 29506, USA
4 Graduate School of Horticulture, Chiba University, Matsudo, 271-8510, Japan
5 University of Chinese Academy of Sciences, Beijing 100049, China

HIGHLIGHTS

- Elevated CO_2 increased the amounts of rhizodeposits.
- The turnover of rhizodeposits derived from N soil was faster than no N soil.
- Rhizodeposits derived from elevated CO_2 decomposed slower than from ambient air.
- Microaggregates and silt-clay were the most and least affected fractions separately.

GRAPHICAL ABSTRACT

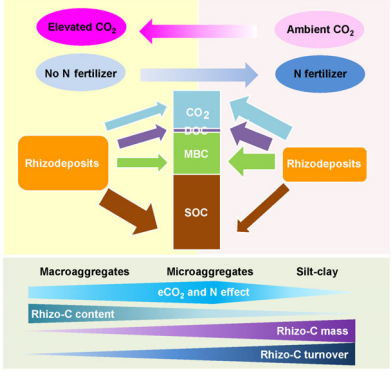

ARTICLE INFO

Article history:
Received December 6, 2019
Revised September 12, 2020
Accepted September 21, 2020

Keywords:
Rice rhizodeposits
Isotope labeling
Aggregates
Elevated carbon dioxide
Nitrogen fertilizer

ABSTRACT

Rhizodeposits in rice paddy soil are important in global C sequestration and cycling. This study explored the effects of elevated CO_2 and N fertilization during the rice growing season on the subsequent mineralization and retention of rhizodeposit-C in soil aggregates after harvest. Rice (*Oryza sativa* L.) was labeled with $^{13}CO_2$ under ambient (400 ppm) and elevated (800 ppm) CO_2 concentrations with and without N fertilization. After harvest, soil with labeled rhizodeposits was collected, separated into three aggregate size fractions, and flood-incubated for 100 d. The initial rhizodeposit-^{13}C content of N-fertilized microaggregates was less than 65% of that of non-fertilized microaggregates. During the incubation of microaggregates separated from N-fertilized soils, 3%–9% and 9%–16% more proportion of rhizodeposit-^{13}C was mineralized to $^{13}CO_2$, and incorporated into the microbial biomass, respectively, while less was allocated to soil organic carbon than in the non-fertilized soils. Elevated CO_2 increased the rhizodeposit-^{13}C content of all aggregate fractions by 10%–80%, while it reduced cumulative $^{13}CO_2$ emission and the bioavailable C pool size of rhizodeposit-C, especially in N-fertilized soil, except for the silt-clay fraction. It also resulted in up to 23% less rhizodeposit-C incorporated into the microbial biomass of the three soil aggregates, and up to 23% more incorporated into soil organic carbon. These results were relatively weak in the silt-clay fraction. Elevated CO_2 and N fertilizer applied in rice growing season had a legacy effect on subsequent mineralization and retention of rhizodeposits in paddy soils after harvest, the extent of which varied among the soil aggregates.

* Corresponding author
E-mail address: yuanhongzhao@isa.ac.cn (H. Yuan)

1 Introduction

In rice (*Oryza sativa* L.) paddy soil, rhizodeposition is an important source of soil organic carbon (SOC) (Kuzyakov, 2002). Rhizodeposits consist of root exudates, sloughed-off cells, mucilage, tissues, cell lysates, and root debris (Kuzyakov and Larionova, 2005; Gregory, 2006), accounting for over 10% of photosynthesized C (Jones et al., 2009; Nguyen, 2009). They contribute 1.5- to 3-fold more C than shoots (Hooker et al., 2005) and represent approximately 26% of the total belowground C input (Liu et al., 2019b). This organic C is often readily available for microorganisms and has a high turnover rate (Kuzyakov, 2002). However, rhizodeposits can also be stabilized by physical (aggregation), chemical (e.g., SOC-mineral interaction), and microbial processes (assimilated into the biomass and humified) and preserved as SOC (Six et al., 2002; Cotrufo et al., 2013; Wei et al., 2019; Cui et al., 2020). Recent studies have reported significant increases in SOC in paddy soil (Pan et al., 2004; Wu, 2011), largely due to the practice of residue incorporation and enhanced belowground C inputs (i.e., root and rhizodeposits) (Lu et al., 2002, 2003).

Climatic changes such as CO_2 elevation and nutrient management such as N fertilization, can influence rhizodeposition and C retention in soils. Elevated CO_2 can increase root biomass and exudates, and augment the root to shoot ratio, enhancing rhizodeposition (Ziska et al., 1996; Bhattacharyya et al., 2013; Zhao et al., 2019). Elevated CO_2 has also been reported to decrease total free amino acids, proline and abscisic acid in root exudates of barley (Calvo et al., 2017) that have relatively great potential to be retained by soil minerals (Keiluweit et al., 2015). In addition, elevated CO_2 increases the C:N ratio of root exudates by decreasing N-rich and increasing C-rich metabolites (Tarnawski and Aragno, 2006). Therefore, rhizodeposits produced under elevated CO_2 conditions have greater potential to be preserved in the soil than to be lost via mineralization. N fertilization also stimulates plant C assimilation, root and shoot biomass production, and rhizodeposition (Kuzyakov, 2002; Ge et al., 2015; Atere et al., 2017; Liu et al., 2019a, Wu et al., 2019; Xiao et al., 2019). Additionally, N fertilization may positively affect N-rich metabolites and have a negative effect on C-rich metabolites, decreasing the C:N ratio of root exudates (Zhen et al., 2016); it may also accelerate the microbial mineralization of rhizodeposits by changing the quality of rhizodeposits and soil C:N ratios, resulting in less C preservation (Li et al., 2017; Zhu et al., 2018; Xiao et al., 2019; Wei et al., 2020). Previous studies have focused primarily on factors influencing the retention and turnover of rhizodeposits during the crop growing season without considering of the fate of the residual rhizodeposits after the harvest (i.e., legacy rhizodeposits) (Ge et al., 2019; Xiao et al., 2019; Zang et al., 2019). However, the rhizodeposit-C remaining after harvest is essential for SOC preservation.

The retention of rhizodeposits in different soil aggregates may vary due to differences in size, stability, capacity to preserve C (Six et al., 2002), and the accessibility of C to microorganisms (von Lützow et al., 2007; Brookes et al., 2017). This can be crucial for rhizodeposit-C sequestration (von Lützow et al., 2007; Schmidt et al., 2011). Several studies and models have suggested that macroaggregates contain fresh C inputs with short residence times (Elliott, 1986; Six et al., 2002), while microaggregates and silt-clay size aggregates accumulate SOC with longer residence times (Oades, 1988; Denef et al., 2007); others have reported that C input is preferentially sequestered in microaggregates and silt-clay within macroaggregates (Kong et al., 2005; Smith et al., 2014). Pan et al. (2008) reported that in paddy soils, SOC preferentially accumulated in the macro- and microaggregates, while Atere et al. (2017) found a greater deposition of photosynthesized C in silt-clay size aggregates. This divergence may be associated with the effects of different field practices on aggregate formation (Brye et al., 2012; Choudhury et al., 2014). Despite the conflicting results, these studies highlight the importance of soil aggregates in C retention. However, information on the turnover and retention of legacy rhizodeposits associated with soil aggregates is quite limited.

The objective of the present study was to reveal the legacy effect of elevated CO_2 and N fertilization on the fate of legacy rhizodeposit-C by analyzing the decomposition and retention of legacy rhizodeposit-C derived from rice grown under conditions with and without elevated CO_2 and N fertilization. It was hypothesized that (1) legacy rhizodeposits remaining after the rice growing season are preferentially retained in macroaggregates and are less mineralizable than those retained in microaggregates and silt-clay fractions; and (2) legacy rhizodeposits derived from rice grown under elevated CO_2 conditions are less mineralizable and are preferentially retained in soil aggregates, whereas legacy rhizodeposits derived from rice grown with N fertilization should exhibit the opposite characteristics.

2 Materials and methods

2.1 ^{13}C-CO_2 continuous labeling

Typical paddy soil was sampled for the pot experiment at the Changsha Research Station for Agricultural and Environmental Monitoring, Hunan, China (113°19′52″ E, 28°33′04″ N; 80 m above sea level). The area is characterized by a subtropical climate, with a mean annual temperature of 17.5°C and an annual rainfall of 1300 mm. The soil (sand 16.5%, silt 73.5%, and clay 10.0%) was collected from 0 to 20 cm depth. The soil (pH 6.4, 1:2.5 w:v) contained 27.10 g kg^{-1} total organic carbon, 2.60 g kg^{-1} total nitrogen, and 0.74 g kg^{-1} total phosphorus. Rhizodeposit labeling was conducted as described by Ge et al. (2013). Each pot (17.2 cm diameter, 16.7 cm height) was filled with soil, equivalent to 1.2 kg dry weight. After applying base fertilizers (KH_2PO_4 20 mg P kg^{-1} soil, KCl 120 mg K kg^{-1} soil), three rice seedlings were planted in each pot, and the soil was flooded with water 3 cm deep. The pots were then transferred to

automatically-controlled, gas-tight growth chambers (150 cm length, 100 cm width, 150 cm height).

There were four treatments: ambient CO_2 level (400 ppm) and no N fertilizer (AN_0); elevated CO_2 level (800 ppm) and no N fertilizer (EN_0); ambient CO_2 level and 100 mg N kg^{-1} (equivalent to 225 kg N ha^{-1}) (AN_{100}); and elevated CO_2 level with 100 mg N kg^{-1} (EN_{100}). CO_2 was generated by acidifying Na_2CO_3 (in beakers placed inside the growth chambers), with 0.5 M H_2SO_4, and the concentration was monitored using a CO_2 analyzer (Shsen-QZD, Qingdao, China). When the CO_2 concentration in the chamber fell below 100 μL L^{-1}, CO_2 was generated to maintain a concentration of 380–400 or 780–800 μL L^{-1}; when it rose above 400 or 800 μL L^{-1}, a switch diverted the gas to pass through CO_2 traps (1 M NaOH solution) to absorb the excess CO_2. During the tillering an – d elongation stages (a 43 d period), the CO_2 was continuously labeled with 2.8 atom% ^{13}C, and the beaker was filled with $Na_2{}^{13}CO_3$ every 6 d (1.0 M, 99 atom% ^{13}C; Cambridge Isotope Laboratories, Tewksbury, MA, USA). The urea-N fertilizer was separated into three portions in a ratio of 5:3:2 to apply at the seedling, tillering, and heading stages. After the rice harvest, the soil was collected, and the total C content and ^{13}C atom% of the different soil particle fractions and bulk (unfractionated) soil were determined. The natural abundance was obtained by the same process but without ^{13}C labeling.

2.2 Soil particle fractionation and incubation setup

After 150 d, the rice was harvested, and the soil was collected. Plant roots and leaves in the soil were carefully removed by handpicking. The soil was sequentially wet-sieved with distilled water into macroaggregate (>250 μm), microaggregate (53–250 μm), and silt and clay (< 53 μm) fractions as described by Atere et al. (2017) and dried overnight at 50°C.

The bulk soil and fractionated particle fractions collected from the four treatments (AN_0, EN_0, AN_{100}, and EN_{100}) were used to conduct an incubation experiment. Approximately 20 g soil was transferred into a 500 mL glass bottle, flooded with water 2 cm deep, sealed with a rubber stopper, and kept for 100 d at 25°C. Using a gas-tight syringe, approximately 30 mL headspace gas was sampled every day for the first 15 days and then every 2–10 days thereafter, until the end of the experiment. The samples were stored in pre-evacuated Exetainer glass bottles (Labco, High Wycombe, UK); the glass bottles were kept closed between the sampling dates and were only opened for ~30 min each sampling day to be aired with atmospheric air for aerobic maintenance. The CO_2 concentration and $^{13}CO_2$ atom% were determined. The soil was destructively sampled on days 5, 30, and 100 for further measurements.

2.3 CO_2 efflux, microbial biomass carbon and ^{13}C isotope analysis

CO_2 concentrations of the headspace gas samples were measured using a gas chromatographer (Agilent 7890A; Agilent Technologies, Palo Alto, CA, USA) equipped with a thermal conductivity detector. The stable C isotope composition of CO_2 in the headspace gas samples was analyzed using an isotope ratio mass spectrometer coupled with a GasBench (Thermo–Fisher Scientific, Waltham, MA, USA). The soil microbial biomass C (MBC) of the bulk soil and aggregate samples was measured following the fumigation extraction method (Wu et al., 1990). The equivalent of 15 g dry soil was extracted with 60 mL of 0.05 M K_2SO_4. Another 15 g dry soil sample was fumigated with alcohol-free $CHCl_3$ for 24 h and extracted in the same manner. The MBC was calculated based on the difference in dissolved organic C (DOC) between the fumigated and non-fumigated samples, using a K_{EC} factor of 0.45 (Wu et al., 1990). The mineral N (NH_4^+ and NO_3^-) content in the same non-fumigated extract was measured. Extracts of fumigated and non-fumigated samples were freeze-dried and subsequently subjected to $\delta^{13}C$ analysis. Soils were mixed thoroughly, and a subsample (10 g) was air-dried and ball-milled before total C and $\delta^{13}C$ analyses. The stable C isotope composition of the soils and freeze-dried extracts was analyzed using a MAT253 isotope ratio mass spectrometer (Thermo–Fisher Scientific, Waltham, MA, USA) coupled with a FLASH 2000 elemental analyzer (Thermo–Fisher Scientific). Total C was analyzed using a TOC-VWP total C analyzer (Shimadzu, Kyoto, Japan).

2.4 Calculation and statistics

The $\delta^{13}C$ values of the soil with labeled rhizodeposits and CO_2 were converted into δ (‰) relative to the Pee Dee Belemnite (PDB, 0.0111802) standard and further expressed in atom% as follows:

$$\text{atom}\,\% = 100 * 0.0111802 * \left(\frac{\delta}{1000} + 1\right) / \left(1 + 0.0111802 * \left(\frac{\delta}{1000} + 1\right)\right). \quad (1)$$

The ^{13}C content (mg kg^{-1}) of DOC, SOC and CO_2 levels were calculated using the following equation:

$$^{13}C_{\text{content}} = (\text{atom}\,\%_{\text{sample}} - \text{atom}\,\%_{\text{natural}}) * C_{\text{sample}}/100, \quad (2)$$

where $\text{atom}\%_{\text{sample}}$ and $\text{atom}\%_{\text{natural}}$ are the atom% ^{13}C in the labeled and unlabeled sample, respectively, and C_{sample} is the total C content (mg kg^{-1}) of the sample. The $^{13}CO_2$ content was calculated using an analog equation. The SOC-^{13}C content measured before incubation was assumed to be all sourced from rhizodeposits and is referred to as the initial rhizodeposit-^{13}C content.

The allocation of rhizodeposit-^{13}C of the bulk soil and aggregates (macroaggregates, microaggregates, and silt-clay) into different pools (CO_2, DOC, MBC, and SOC) was calculated as follows:

$$\text{DOC Proportion}_{\text{bulk}} = {}^{13}\text{DOC}_{\text{bulk}}/\text{Rhizo-}{}^{13}\text{C}_{\text{bulk}} * 100\%. \quad (3)$$

$\text{DOC Proportion}_{\text{bulk}}$ (%) is the proportion of initial rhizodeposit-^{13}C content transformed into ^{13}C-DOC in the bulk soil; $^{13}\text{DOC}_{\text{bulk}}$ (mg kg^{-1}) is the ^{13}C-DOCcontent of the bulk soil. Rhizo-$^{13}\text{C}_{\text{bulk}}$ (mg kg^{-1}) is the initial rhizodeposit-^{13}C content

of the bulk soil before the start of incubation. The proportion of DOC in macroaggregates, microaggregates, and silt-clay was calculated using the same equation. The proportion of rhizodeposit-^{13}C content transformed into ^{13}C-MBC, ^{13}C-CO_2, and ^{13}C-SOC was calculated using the analog equation.

The cumulative $^{13}CO_2$ emission was calculated as follows:

$$\text{Cumulative } {}^{13}CO_2 = \Sigma_1^n {}^{13}CO_{2t} * 100/{}^{13}C_{\text{initial}}, \quad (4)$$

where cumulative $^{13}CO_2$ is the cumulative $^{13}CO_2$ emission (% of the initial ^{13}C-SOC content); n represents the incubation time (days); $^{13}CO_{2t}$ is the ^{13}C-CO_2 efflux (mg kg^{-1} d^{-1}) at day t; $^{13}C_{\text{initial}}$ is the initial rhizodeposit-^{13}C content of each aggregate (mg kg^{-1}) of the soil before incubation.

The kinetics of the mineralization was described by fitting a first-order single exponential function:

$$^{13}C_{\min} = b(1 - e^{-kt}), \quad (5)$$

where b describes the amount of bioavailable labeled rhizodeposits pool, k is the mineralization rate of the pool of rhizodeposits, and t is time (days). The parameters obtained were used to calculate the mean residence time (MRT) as 1/k, and half-life as ln2/k (Zhu et al., 2016).

Statistical comparisons between treatments within the same aggregate fraction or between aggregate fractions within the same CO_2 and N treatment were performed using analysis of variance with Tukey pairwise post-hoc testing, and effects were considered significant at $p < 0.05$. A two-factorial analysis of variance (ANOVA) was conducted on rhizodeposit-^{13}C content, cumulative CO_2 emission, ^{13}C-MBC, ^{13}C-DOC and ^{13}C-SOC proportions with the factors of elevated CO_2 concentration and N fertilization. Pearson's correlation was conducted between daily ^{13}C-CO_2, ^{13}C-MBC, and ^{13}C-DOC proportions and soil physicochemical parameters in each aggregate with data from three soil sampling dates. Statistical analyses were conducted using SPSS v22 (IBM Inc., Armonk, NY, USA).

3 Results

3.1 Aggregate distribution and associated C

The recovery of aggregates measured by wet-sieving was 91%–99% for dry weight, 85%–114% for SOC, and 60%–88% for rhizodeposit-^{13}C (Figs. 1A, B, C). The silt-clay fraction accounted for the largest proportion of dry weight, SOC, and rhizodeposit-^{13}C of soil (79%–83%, 65%–74%, and 37%–58%, respectively), followed by the microaggregate fraction (10%–12%, 17%–22%, and 10%–17%, respectively) (Figs. 1A, B, C). Elevated CO_2 increased the mass and SOC proportion of macroaggregates in bulk soil ($p < 0.05$) and decreased the rhizodeposit-^{13}C proportion of the silt-clay fraction in bulk soils ($p < 0.05$). N fertilization increased the rhizodeposit-^{13}C proportion in the silt-clay fraction but decreased it in the microaggregates ($p < 0.05$) (Fig. 1C).

In contrast to its mass distribution, the rhizodeposit-^{13}C content of each fraction declined with decreasing aggregate size (Fig. 2A, B). The interactions between elevated CO_2 and N fertilization were observed in the rhizodeposit-^{13}C contents of the bulk soils and microaggregates (Online Resource 2). Elevated CO_2 increased the rhizodeposit-^{13}C content of bulk soil and all aggregate fractions by 10%–80% (for the comparisons between AN_0 vs. EN_0 and AN_{100} vs. EN_{100}) ($p < 0.05$). In contrast, N fertilization reduced the content in bulk soils and microaggregates under elevated CO_2 conditions by 24% and 36%, respectively, (for the comparisons between EN_0 vs. EN_{100}) ($p < 0.05$) (Online Resource 2; Fig. 2B). Similarly, N fertilization under ambient CO_2 conditions reduced the rhizodeposits in microaggregates by 37%

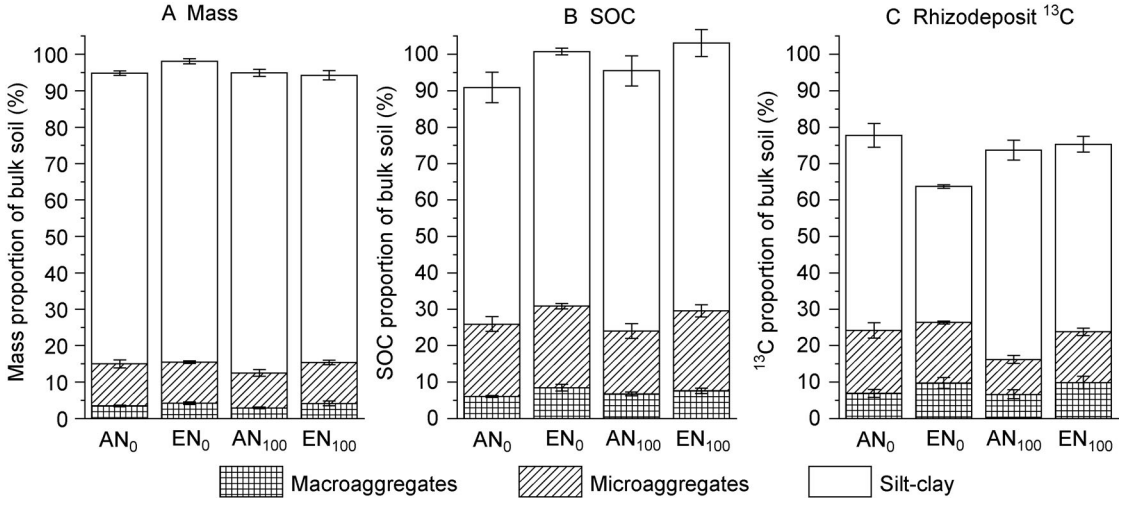

Fig. 1 Distribution of (A) mass, (B) soil organic carbon (SOC), and (C) rhizodeposit-^{13}C of the bulk soil in different aggregates after rice growth under ambient CO_2 concentration without N fertilization (AN_0), elevated CO_2 concentration without N fertilization (EN_0), ambient CO_2 concentration with N fertilization of 100 mg N kg^{-1} soil (AN_{100}), and elevated CO_2 concentration with N fertilization of 100 mg N kg^{-1} soil (EN_{100}) treatments. All data are means±SE (n = 3).

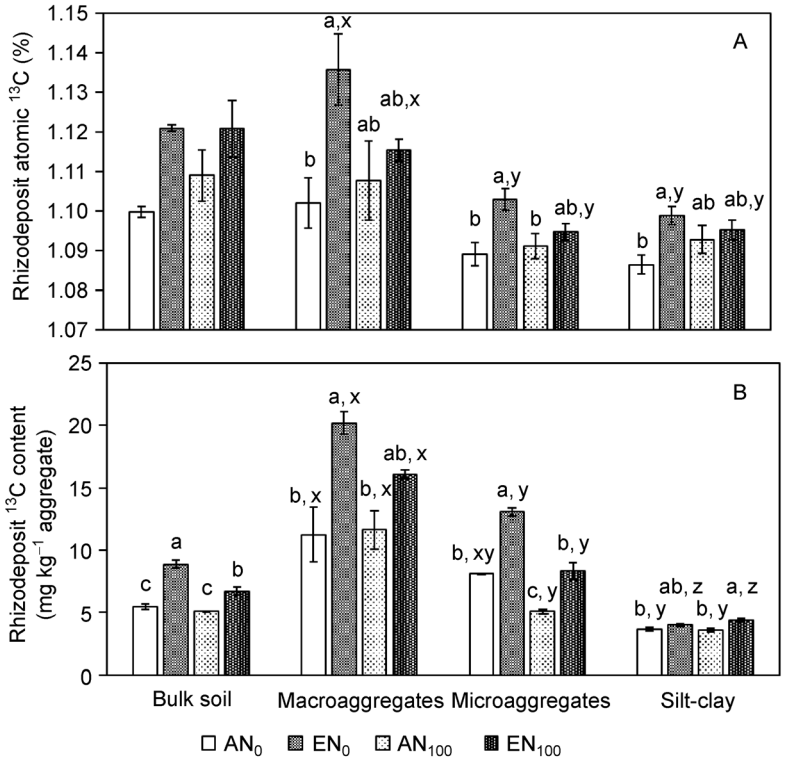

Fig. 2 Rhizodeposit-^{13}C values (atom%) (A), and content (mg kg^{-1}) (B) of bulk soil and soil aggregate fractions after rice growth in treatments AN_0, EN_0, AN_{100}, and EN_{100}. All data are means±SE (n = 3). Lowercase letters a, b, and c indicate significant differences ($p < 0.05$) of the measured parameters between different treatments within the same aggregate fraction, and x, y, and z indicate significant differences ($p < 0.05$) of the measured parameters between aggregate size fractions within the same treatment. The y-axis in (A) starts from the natural abundance value of 1.072% measured in the soil without ^{13}C isotope labeling.

(for the comparisons between AN_0 vs. AN_{100}) ($p < 0.05$), but had no effect on the other two fractions.

3.2 Mineralization of rhizodeposit-^{13}C

On day 5, when the most easily consumable C compounds existed and were being preferentially used, the rhizodeposit mineralization rate was fast, and 0.8%–1.0% of rhizodeposit-^{13}C in macroaggregates of all treatments was mineralized to CO_2. The cumulative $^{13}CO_2$ emission on day 5 increased with decreasing aggregate sizes (1.2%–2.2% of microaggregates, 2.1%–2.8% of silt-clay) (Fig. 3). The cumulative $^{13}CO_2$ emission of all aggregate fractions showed greater mineralization in N-fertilized soil (AN_{100} and EN_{100}) than non-fertilized soil (AN_0 and EN_0) on day 5 ($p < 0.05$). In the silt-clay fraction, cumulative $^{13}CO_2$ emission from the treatment of elevated CO_2 (EN_0 and EN_{100}) was higher than the ambient CO_2 treatment (AN_0 and AN_{100}) on day 5 but was opposite in the microaggregates. At the end of the experiment (100 d), 12%–25% of rhizodeposit-^{13}C had been mineralized (Fig. 3), thus exceeding the level of SOC mineralization ($p < 0.05$) (Online Resource 1) and suggesting that rhizodeposit-C is more labile and available to soil microorganisms.

In the bulk soil, macroaggregates, and microaggregates, cumulative $^{13}CO_2$ emission at the end of incubation (100 d) was higher in the N treatments (AN_{100} and EN_{100}) than in treatments with no N fertilizer (AN_0 and EN_0) ($p < 0.05$); 3%–9% more rhizodeposits were mineralized to CO_2 in N-fertilized soil. In N-fertilized soil, the treatment with elevated CO_2 showed lower cumulative $^{13}CO_2$ emission at the end of incubation than the treatment with ambient CO_2 in the bulk soil, macroaggregates, and microaggregates ($p < 0.05$), but it was the opposite in the silt-clay fraction ($p < 0.05$) (Fig. 3). In the non-fertilized soil, the cumulative $^{13}CO_2$ emission at the end of the experiment was in the order of silt-clay>microaggregates>macroaggregates, whereas in N-fertilized soil, it was highest in the microaggregates and lowest in macroaggregates (Fig. 3).

The cumulative $^{13}CO_2$ emission fitted to the first-order kinetic model [Eq. (5)], and the MRT of different aggregate fractions decreased with reducing aggregate size (Table 1). The MRT and bioavailable pool size of rhizodeposit-^{13}C in the aggregate fractions varied across the treatments with elevated CO_2 and N fertilization, which however, was not observed in the bulk soils (Table 1). The rhizodeposits derived from rice grown under elevated CO_2 treatments showed a 25%–51% shorter MRT and a 17%–45% smaller bioavailable C pool size than under ambient CO_2 treatments for all soil fractions ($p < 0.05$), except in macroaggregates without N fertilization and microaggregates with N fertilization (Table 1).

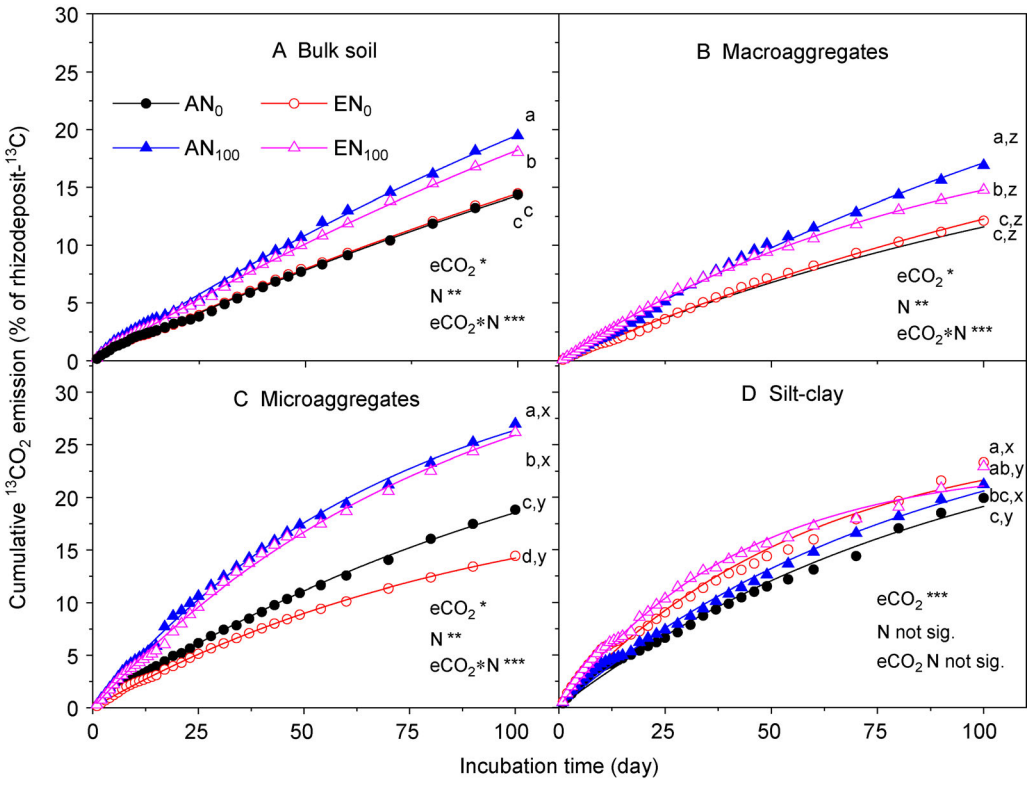

Fig. 3 Cumulative $^{13}CO_2$ emission (% of rhizodeposit-^{13}C) of bulk soil and aggregate fractions in treatments AN_0, EN_0, AN_{100}, and EN_{100}. All data are means±SE (n = 4). Lowercase letters a, b, and c represent significant differences ($p < 0.05$) between treatments within the same aggregate fraction on day 100 of incubation, and x, y, and z indicate significant differences ($p < 0.05$) between different aggregate fractions within the same treatment on day 100 of incubation. Two-factorial analysis of variance (ANOVA) was conducted with the factors of elevated CO_2 concentration (eCO_2) and N fertilization (N) on cumulative CO_2 emission at the end (100 d) of incubation. *, **, and *** indicate significance levels of $p < 0.05$, $p < 0.01$ and $p < 0.001$, respectively. Not sig. indicates the effect is not statistically significant. The curves are fitted to a first-order single exponential Eq. (5).

Rhizodeposits from rice grown in the N-fertilized soil showed a 9%–52% shorter MRT than non-fertilized soil in all aggregates under elevated CO_2 conditions and 42% shorter in microaggregates under ambient CO_2 conditions ($p < 0.05$) (Table 1). Rhizodeposits in macroaggregates from N-fertilized soil showed a larger bioavailable pool than the non-fertilized soil under ambient CO_2 conditions, and microaggregates under elevated CO_2 conditions; while in macroaggregates and silt-clay under elevated CO_2 conditions, the non-fertilized soil showed a larger bioavailable pool of rhizodeposits (Table 1). Cumulative $^{13}CO_2$ emission was correlated with soil MBC, NH_4^+, SOC, soil organic nitrogen (SON) content, and SOC/SON (Table 2). The daily $^{13}CO_2$ emission rate was correlated with the DOC content and ^{13}C-DOC proportion; NH_4^+; pH; SOC and SON content; and SOC/SON (Table 2).

3.3 Rhizodeposit-^{13}C retention

On day 5, when the rhizodeposit mineralization was fastest, the proportion of rhizodeposit-^{13}C incorporated into DOC tended to increase with decreasing aggregate size (Fig. 4), which was consistent with mineralization (Fig. 3), while the ^{13}C-SOC proportion showed the opposite trend. For incorporation of rhizodeposit-^{13}C into MBC on day 5, microaggregates generally had a larger ^{13}C-MBC proportion (16%–31%) than the other two aggregate fractions (4%–9% in macroaggregates, and 11%–18% in silt-clay) (Fig. 4).

On day 5, elevated CO_2 increased the proportion of ^{13}C-MBC in microaggregates relative to ambient CO_2 in non-fertilized soil ($p < 0.05$). In the silt-clay fraction, both elevated CO_2 and N fertilization had a positive effect on the ^{13}C-MBC proportion ($p < 0.05$) (Online Resource 5). N fertilization with elevated CO_2 had significant effects and interaction effects on the incorporation of rhizodeposit-^{13}C into DOC in all three aggregate fractions on day 5 (Online Resource 5). On day 5, the proportion of ^{13}C-DOC in N-fertilized soil under elevated CO_2 treatment was greater than the other treatments in all soil fractions ($p < 0.05$), and it decreased sharply from day 5 to day 30 (Fig. 4). In macroaggregates, only the ^{13}C-DOC proportion in the treatment with both elevated CO_2 and N fertilization significantly increased over time (Fig. 4). Along with the mineralization of rhizodeposit-^{13}C, its incorporation into SOC decreased over time in all treatments of the aggregate fractions and bulk soil (Fig. 4).

At the end of the incubation period (100 d), 5%–44% of the initial rhizodeposit-^{13}C of each aggregate was in MBC and 31%–83% and < 0.19% were in SOC and DOC, respectively (Fig. 4). At 100 d, N fertilization and elevated CO_2 had no

effect on the proportions of ^{13}C-DOC and ^{13}C-MBC in macroaggregates or the silt-clay fraction (Online Resource 5). For the treatment with N fertilization only, in microaggregates, 2%–5% and 9%–16% increases in rhizodeposits were recorded in DOC and MBC, respectively, over the same in the treatment without N fertilization, especially under ambient CO_2 conditions (Fig. 4). These increases were in contrast to the ^{13}C-SOC proportion (Fig. 4). Rhizodeposit-^{13}C derived from elevated CO_2 showed 0.01%–0.14% and 0.1%–22.5% decreased incorporation into the DOC and MBC pools, respectively and 2.8%–23.3% increased incorporation into SOC (in aggregate fractions of both N-fertilized and non-fertilized soils) ($p < 0.05$), except for macroaggregates (Fig. 4). On day 100, elevated CO_2 and N fertilization showed positive interactions on the proportions of ^{13}C-DOC and ^{13}C-MBC but a negative interaction on the proportion of ^{13}C-SOC in the silt-clay fraction ($p < 0.05$) (Online Resource 5).

4 Discussion

4.1 Distribution of rhizodeposit-C in soil aggregates

Rhizodeposits derived from the early growth stage are primarily labile substrates such as exudates, while during the later growth stage, they are relatively more recalcitrant substances of root turnover products, such as sloughed-off cortical cells, fine roots, and senescent root fragments (Aulakh et al., 2001; Jones et al., 2004). Microbial utilization of those labile rhizodeposit substrates is very swift, i.e., within a few hours (Kuzyakov and Jones, 2006; Fischer and Kuzyakov, 2010; Fischer et al., 2010), while for relatively recalcitrant substrates, this consumption could take days (Dormaar, 1992). Pausch et al. (2013) reported that 62% of rhizodeposition was mineralized within 16 days of maize growth. Therefore, the most labile forms of rhizodeposits may have

Table 1 Mean residence time (MRT) and bioavailable pool size of rhizodeposit-^{13}C in bulk soil and particle size fractions in AN_0, EN_0, AN_{100} and EN_{100} treatments. Cumulative $^{13}CO_2$ emission values were fitted to the first order kinetics: $^{13}C_{min} = b\,(1 - e^{-kt})$. MRT = 1/$k$. All data are means±SE (n = 4).

Treatment[a]	MRT (day)				Size (%)			
	Bulk soil	Macroaggregates	Microaggregates	Silt-clay	Bulk soil	Macroaggregates	Microaggregates	Silt-clay
AN	259	149 b,x	124 a,y	95 a,z	45	24 c,y	31 b,x	29 a,x
EN	261	184 a,x	93 b,y	58 b,z	46	29 b,x	22 c,y	24 b,xy
AN	224	177 a,x	72 d,y	86 a,y	54	40 a,x	32 ab,y	27 a,y
EN	231	88 c,x	84 c,x	42 c,y	52	22 c,y	34 a,x	21 c,y
eCO_2	0.82	< 0.001	< 0.001	< 0.001	0.85	< 0.001	< 0.001	< 0.001
N fertilisation	0.12	< 0.001	< 0.001	< 0.001	0.04	< 0.001	< 0.001	0.002
eCO_2*N fertilisation	0.89	< 0.001	< 0.001	0.091	0.64	< 0.001	< 0.001	0.58

[a]AN_0, treatment with ambient CO_2 concentration without N fertilisation; EN_0, treatment with elevated CO_2 concentration without N fertilisation; AN_{100}, treatment with ambient CO_2 concentration and N fertilisation at 100 mg N kg^{-1} soi; EN_{100}, treatment with elevated CO_2 concentration and N fertilisation at 100 mg N kg^{-1} soil.Lowercase letters a, b, and c after numerical values indicate significant differences ($p < 0.05$) between different treatments within the same aggregate fraction, and x, y, and z indicate significant differences ($p < 0.05$) between different aggregate fractions within the same treatment.

Table 2 Pearson's correlation coefficients between ^{13}C-CO_2, ^{13}C-MBC, ^{13}C-DOC (% of rhizodeposit-^{13}C) and aggregates properties.

	Daily $^{13}CO_2$	^{13}C-MBC	^{13}C-DOC	DOC	MBC	MBN	NH_4^+	pH	SOC	SON	MBC/MBN	SOC/SON
Cumulative $^{13}CO_2$	**−0.613**[**a]	**0.341***	−0.206	−0.257	**0.303***	−0.105	**−70.63****	0.17	**0.592****	**0.389****	0.23	**0.762****
Daily $^{13}CO_2$		0.236	**0.576****	**0.473****	−0.01	0.122	**0.731****	**−0.360***	**−0.563****	**−0.478****	−0.105	**−0.561****
^{13}C-MBC			0.242	0.139	**0.673****	0.169	−0.029	0.038	0.104	0.108	0.224	0.110
^{13}C-DOC				**0.940****	−0.145	**0.318***	0.249	−0.258	−0.114	−0.153	−0.243	0.010

[a]* and ** indicate significant correlation at $p < 0.01$ and $p < 0.05$, respectively. DOC, dissolved organic carbon; MBC, microbial biomass carbon; MBN, microbial biomass nitrogen; SOC, soil organic carbon; SON, soil organic nitrogen.

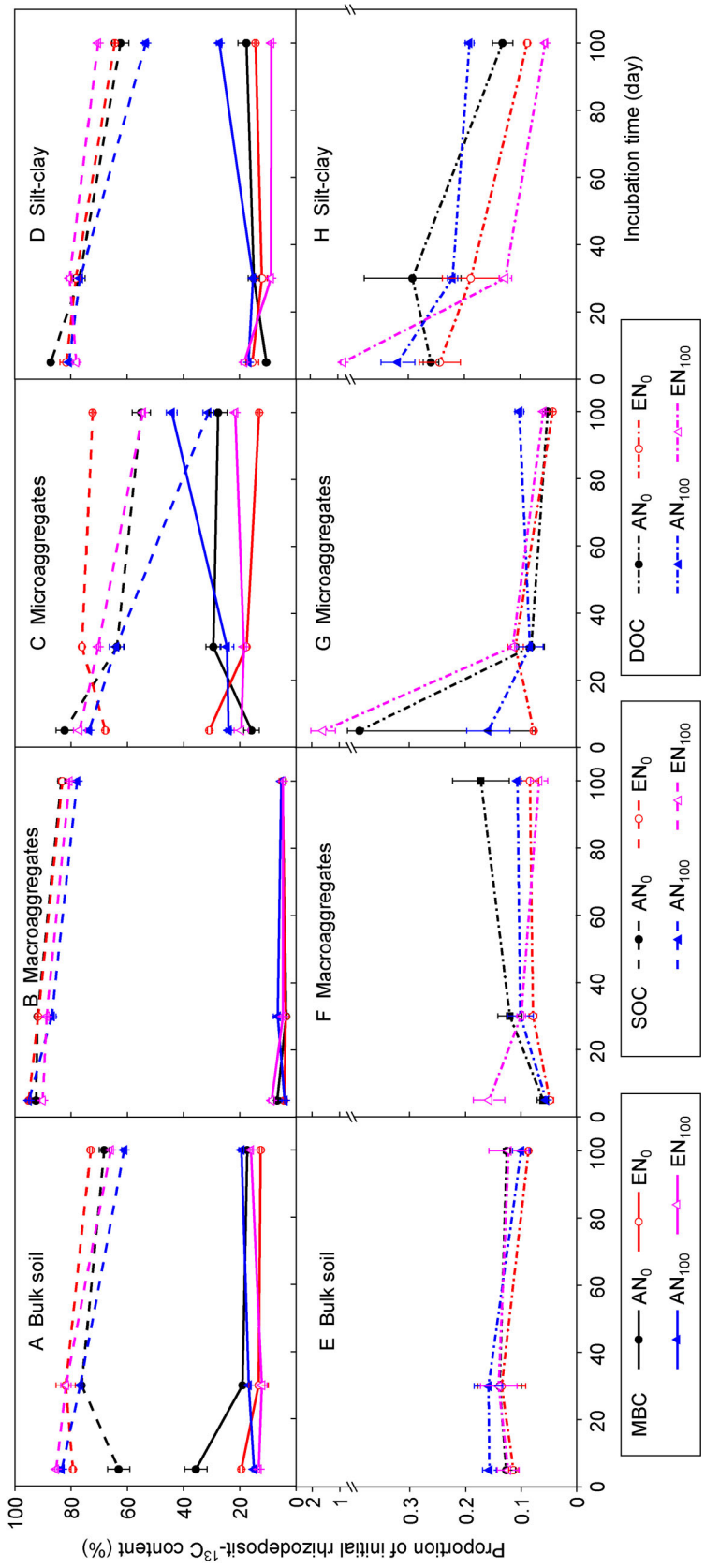

Fig. 4 Proportion of rhizodeposit-^{13}C allocated to microbial biomass C (MBC) (A–D), dissolved organic C (DOC) (E–H) and soil organic C (SOC) (A–D) of bulk soil and soil aggregate fractions during incubation under treatments of AN_0, EN_0, AN_{100} and EN_{100}. All data are means±SE (n = 3)

been lost during rice growth, and the legacy rhizodeposits we studied were the less labile forms. During the separation of the aggregates by the wet-sieving method, 22%–36% of rhizodeposit-^{13}C was lost. In contrast, the recovery rates of SOC and dry weight for the wet-sieving method were quite high (>85%) (Fig. 1). Previous studies have also reported approximately 90% SOC recovery after wet-sieving (Lopez-Sangil and Rovira, 2013; Zou et al., 2015). These suggest that the lost rhizodeposit-^{13}C may be mainly in dissolved forms, and this did not influence our study on the distribution, transformation, and fate of rhizodeposit-C within the aggregates.

Rhizodeposit-^{13}C content was highest in macroaggregates, followed by microaggregates and silt-clay (Fig. 2B). $^{13}CO_2$ emission was slower from macroaggregates than microaggregates and the silt-clay fraction (Fig. 3, Table 1). This result was consistent with our first hypothesis that rhizodeposit-C is preferentially retained in macroaggregates and is less mineralizable than in other finer fractions. Roots are preferentially located between and within large macroaggregates under flooding conditions during the rice growing season to allow for greater atmospheric O_2 exchange than if they were within and between microaggregates (Luo et al., 2018). However, due to O_2 conditions, more mineralizable organic materials in macroaggregates decomposed relative to the smaller aggregates during rice growth.

Moreover, the protection of organic matter in microaggregates is stronger than in macroaggregates (Six et al., 2002; von Lützow et al., 2007). This resulted in the preservation of relatively more recalcitrant/well-decomposed rhizodeposits in macroaggregates at the beginning of the incubation period. Furthermore, the macroaggregates' MBC content was generally the lowest (Online Resource 4) because of its lower surface area and reduced habitat for microorganisms, resulting in the slowest mineralization of rhizodeposits in paddy soil. Due to alternate flooding and drying, and tillage practices, it is difficult for macroaggregates to be formed and maintained. Smaller-sized fractions, i.e., silt-clay, accounted for a larger proportion of the soil mass; therefore, higher proportions of rhizodeposit-C and SOC were found in the silt-clay fraction (Fig. 1C).

Rice rhizodeposition was greater in treatments with elevated CO_2 than with ambient CO_2 (Fig. 1) that can be attributed to increased photosynthesis (Bhattacharyya et al., 2013); this corroborates the results of studies on other plants (Pendall et al., 2004; Allard et al., 2006; Phillips et al., 2011; Calvo et al., 2017). Elevated CO_2 stimulates root growth, mucilage and associated fungal hyphae, and encourages the formation of macroaggregates from microaggregates, silt, and clay particles (Czarnes et al., 2000; Traore et al., 2000; Rillig and Mummey, 2006; Jastrow et al., 2007). As a result, we observed an increase in macroaggregate mass (Fig. 1). Regarding the rhizodeposit-^{13}C content, elevated CO_2 had a positive effect on bulk soil and all aggregate fractions, but to varying degrees, the least effect was observed in the silt-clay fractions. Such differences may be the result of particulate organic C derived from root residues being occluded in macroaggregates and microaggregates but not in silt-clay (Six et al., 2002). As a result, silt-clay accounted for a reduced proportion of rhizodeposit-^{13}C in bulk soil due to elevated CO_2.

Although N fertilization stimulates plant photosynthesis, it can lower the root/shoot biomass ratio (Ge et al., 2015; Atere et al., 2017; Luo et al., 2018; Xiao et al., 2019) because fewer root exudates and less root biomass are required when the soil N limitation is mitigated (Britto and Kronzucker, 2002; Linkohr et al., 2002; Li et al., 2010; Ge et al., 2017). As a result, the rhizodeposit-^{13}C content in N-fertilized bulk soil was lower, especially under elevated CO_2 (Fig. 2B). Moreover, N fertilization has been reported to promote C loss via respiration during rice growth (Zhu et al., 2018; Xiao et al., 2019); therefore, more rhizodeposit-^{13}C may have been depleted in the N-fertilized soil before the start of incubation, especially in microaggregates. As a result, the proportion of microaggregates in rhizodeposit-^{13}C of bulk soil was less in the N-fertilized soil than the non-fertilized soil. N fertilization had no impact on aggregate mass distribution in rice paddy soil (Figs. 1, 2), consistent with Luo et al. (2018).

In general, rhizodeposits were preferentially retained in macroaggregates, and these legacy rhizodeposits in macroaggregates were less mineralizable. CO_2 elevation and N fertilization had opposite effects on each aggregate's initial rhizodeposit content; the silt-clay fraction was the least affected.

4.2 Effect of N fertilization on mineralization and retention of rhizodeposit-C associated with soil aggregates

The legacy effect of N fertilization on rhizodeposit mineralization and retention in paddy soil silt-clay was limited except for at the very beginning stage. On day 5, the silt-clay was the only soil fraction showing a larger ^{13}C-MBC proportion in the N-fertilized than non-fertilized soil, indicating microbial immobilization at this early stage. However, considering the entire 100-day incubation period of the silt-clay, the cumulative $^{13}CO_2$ emission and its allocation to DOC and MBC were not influenced by N fertilization (Figs. 3, 4, Online Resource 5). This might be because in the silt-clay, C retention was mainly through binding between minerals and organic substrates that contain functional groups, such as hydroxyls and carboxyls (Cotrufo et al., 2013), without other mechanisms such as the occlusion of particulate organic C from macroaggregates (Six et al., 2002; von Lützow et al., 2007). Since the silt-clay is relatively stable in its content, structure and binding capacity in the soil for only one growing season, N fertilization could hardly alter the rhizodeposit retention processes occurring in it.

Similar to the silt-clay, N fertilization had little effect on the initial rhizodeposit-^{13}C content, and its incorporation in DOC and MBC in macroaggregates (Online Resources 2, 5), but had a positive effect on the cumulative $^{13}CO_2$ emission and the bioavailable pool of its rhizodeposit-C ($p < 0.05$) (Fig. 3, Table 1). These results indicated that N fertilization in

macroaggregates might result in less recalcitrance of the rhizodeposit and greater mineralization for energy, but not for microbial growth. Besides binding between minerals and organic substrates, macroaggregates also occlude free particulate organic C that could explain the difference in the cumulative $^{13}CO_2$ emission resulting from N fertilization.

Microaggregates were the soil fraction most influenced by N fertilization. N fertilization increased cumulative $^{13}CO_2$ emission and the bioavailable pool of rhizodeposit-C in microaggregates (Fig. 3, Table 1). Under ambient CO_2 conditions, in microaggregates, N fertilization increased the allocation of rhizodeposits to DOC and MBC. Microaggregates also occlude free particulate organic substrates. However, due to lower porosity and O_2 of microaggregates relative to macroaggregates under flooding conditions during rice growth, less-decomposed substrates may remain in microaggregates after harvest, which led to greater microbial mineralization and immobilization. In general, N fertilization had a positive legacy effect on rhizodeposit mineralization and microbial immobilization but to varying degrees across different aggregate fractions.

4.3 Effect of elevated CO_2 on mineralization and retention of rhizodeposit-C associated with aggregates

Elevated CO_2 resulted in lower cumulative $^{13}CO_2$ emission than ambient CO_2 levels, especially in N-fertilized soil (except for silt-clay fraction) (Fig. 3), and a reduced bioavailable C pool size of rhizodeposits (Table 1). This result indicated that elevated CO_2 might result in more recalcitrant forms of rhizodeposit-C. Consistent with cumulative $^{13}CO_2$ emission, elevated CO_2 resulted in a lower proportion of rhizodeposit-C incorporated into the DOC and MBC pools; however, it increased incorporation into the SOC in soil aggregates (Fig. 4). This result may be attributed to a change in the recalcitrance of rhizodeposits due to elevated CO_2.

A significant interaction of elevated CO_2 and N fertilization was observed with the cumulative $^{13}CO_2$ emission and bioavailable C pool size of rhizodeposits in macroaggregates and microaggregates ($p < 0.05$) (Fig. 3, Table 1). This interaction may be associated with the C:N ratio of rhizodeposits being altered by elevated CO_2 and N fertilization. Elevated CO_2 can increase the plant:root ratio (Norby et al., 2001; Yang et al., 2011), resulting in nutrient limitation and reduce microbial activity and respiration rate (Recous et al., 1995); while N fertilization has the opposite effect (Leuschner et al., 2013; Wei et al., 2017). It could be speculated that elevated CO_2 and N fertilization had a similar effect on the C:N ratio of rice rhizodeposits, although we could not directly obtain evidence of it. When the C:N ratio of rhizodeposits is optimal for microbes, microbial biomass would grow, benefiting C retention (De Sosa et al., 2018). Thus, CO_2 elevation negatively affected rhizodeposit mineralization and microbial immobilization by altering the quality of the rhizodeposits.

In general, as illustrated in Fig. 5, elevated CO_2 resulted in higher rice rhizodeposition after the growing season because of increased photosynthesis (Bhattacharyya et al., 2013). N fertilization resulted in lower initial rice rhizodeposition due to

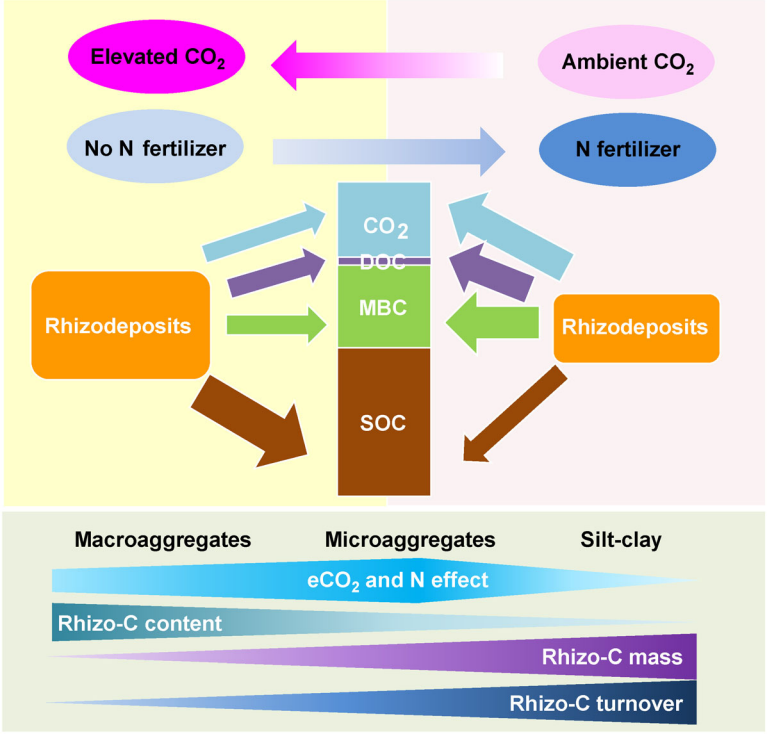

Fig. 5 Conceptual illustration of the effect of CO_2 concentration and N fertilization during rice growing season on the mineralization and allocation of the legacy rhizodeposits in paddy soil aggregate fractions. Thickness of the arrows and squares represents the mass or proportion.

lower allocation of root biomass and exudates and greater mineralization loss during the growing season (Linkohr et al., 2002; Ge et al., 2017; Zhu et al., 2018). Regarding the allocation of legacy rhizodeposits after harvest, rhizodeposits from the elevated CO_2 treatments tended to transfer more to SOC and less to CO_2, DOC and MBC. In contrast, N fertilization tended to result in more rhizodeposits incorporated into CO_2, DOC and MBC, and less into the stable SOC pool. This distribution pattern was mainly associated with the change in the recalcitrance of rhizodeposits caused by elevated CO_2 and N fertilizer during the growing season (Mooshammer et al., 2014). However, the effects of elevated CO_2 and N fertilizer on rhizodeposit mineralization and allocation to different pools was not always significant across the different soil aggregates. The silt-clay had the largest quantity and fastest turnover of rhizodeposits. However, in silt-clay, the change in rhizodeposit mineralization and allocation to different pools due to elevated CO_2 and N fertilizer was quite small, while the change in microaggregates was the largest. This difference was associated with different C preservation mechanisms between the different soil fractions (Six et al., 2002; Kong et al., 2005; von Lützow et al., 2007).

5 Conclusions

The rhizodeposit-^{13}C content decreased with increasing aggregate size, but it was opposite for its distribution proportion in aggregates in all treatments because smaller-sized fractions accounted for a larger proportion of the soil mass. The effect of N fertilization and elevated CO_2 on rhizodeposit mineralization and incorporation into soil organic C pools varied across soil aggregates. N fertilizer increased rhizodeposit mineralization and its incorporation into the soil labile C pools of DOC and MBC, while elevated CO_2 tended to have the opposite effect, although not always significant. The silt-clay was the fraction least affected by the mineralization and retention of legacy rhizodeposit-C, while microaggregates were the most influenced fraction. Therefore, the silt-clay fraction in paddy soil plays a critical and stable role in rhizodeposit-C preservation, while microaggregates have the potential to be regulated and retain more rhizodeposit-C. CO_2 elevation can result in increased preservation of rice rhizodeposit-C, and N fertilizer can cause the legacy rhizodeposit-C to be more mineralizable and less stable.

Acknowledgments

This study was financially supported by the National Key Research and Development Program of China (2017YFD0301504), the National Natural Science Foundation of China (41671292; 41771334; 41877104; 42007097), the Japan-China Scientific Cooperation Program between NSFC and JSPS (41811540031), the Hunan Province Base for Scientific and Technological Innovation Cooperation (2018WK4012), the Innovation Group of Natural Science Foundation of Hunan Province (2019JJ10003), the Natural Science Foundation of Hunan Province for Excellent Young Scholars (2019JJ30028) and the Youth Innovation Team Project of ISA, CAS (2017QNCXTD_GTD). We also thank the Public Service Technology Center, the Institute of Subtropical Agriculture, and the Chinese Academy of Sciences for technical support.

Conflict of interest

The authors declare that they have no conflict of interest.

References

Allard, V., Robin, C., Newton, P.C.D., Lieffering, M., Soussana, J.F., 2006. Short and long-term effects of elevated CO_2 on Lolium perenne rhizodeposition and its consequences on soil organic matter turnover and plant N yield. Soil Biology & Biochemistry 38, 1178–1187.

Atere, C.T., Ge, T., Zhu, Z., Tong, C., Jones, D.L., Shibistova, O., Guggenberger, G., Wu, J., 2017. Rice rhizodeposition and carbon stabilisation in paddy soil are regulated via drying-rewetting cycles and nitrogen fertilisation. Biology and Fertility of Soils 53, 407–417.

Aulakh, M.S., Wassmann, R., Bueno, C., Rennenberg, H., 2001. Impact of root exudates ofdifferent cultivars and plant development stages of rice (*Oryza sativa* L.) on methane production in a paddy soil. Plant and Soil 230, 77–86.

Bhattacharyya, P., Roy, K.S., Neogi, S., Manna, M.C., Adhya, T.K., Rao, K.S., Nayak, A.K., 2013. Influence of elevated carbon dioxide and temperature on below-ground carbon allocation and enzyme activities in tropical flooded soil planted with rice. Environmental Monitoring and Assessment 185, 8659–8671.

Bowsher, A.W., Evans, S., Tiemann, L.K., Friesen, M.L., 2018. Effects of soil nitrogen availability on rhizodeposition in plants: a review. Plant and Soil 423, 59–85.

Britto, D.T., Kronzucker, H.J., 2002. NH_4^+ toxicity in higher plants: a critical review. Journal of Plant Physiology 159, 567–584.

Brookes, P.C., Chen, Y., Chen, L., Qiu, G., Luo, Y., Xu, J., 2017. Is the rate of mineralization of soil organic carbon under microbiological control? Soil Biology & Biochemistry 112, 127–139.

Brye, K.R., Olk, D.C., Schmid, B.T., 2012. Rice rotation and tillage effects on soil aggregation and aggregate carbon and nitrogen dynamics. Soil Science Society of America Journal 76, 994–1004.

Calvo, O.C., Franzaring, J., Schmid, I., Müller, M., Brohon, N., Fangmeier, A., 2017. Atmospheric CO_2 enrichment and drought stress modify root exudation of barley. Global Change Biology 23, 1292–1304.

Choudhury, S.G., Srivastava, S., Singh, R., Chaudhari, S.K., Sharma, D.K., Singh, S.K., Sarkar, D., 2014. Tillage and residue management effects on soil aggregation, organic carbon dynamics and yield attribute in rice–wheat cropping system under reclaimed sodic soil. Soil & Tillage Research 136, 76–83.

Cotrufo, M.F., Wallenstein, M.D., Boot, C.M., Denef, K., Paul, E., 2013. The microbial efficiency matrix stabilization (MEMS) framework integrates plant litter decomposition with soil organic matter stabilization: do labile plant inputs form stable soil organic matter? Global Change Biology 19, 988–995.

Cui, J., Zhu, Z., Xu, X., Liu, S., Jones, D.L., Kuzyakov, Y., Shibistova, O., Wu, J., Ge, T., 2020. Carbon and nitrogen recycling from microbial necromass to cope with C:N stoichiometric imbalance by priming. Soil Biology & Biochemistry 142, 107720.

Czarnes, S., Hallett, P.D., Bengough, A.G., Young, I.M., 2000. Root- and microbial-derived mucilages affect soil structure and water transport. European Journal of Soil Science 51, 435–443.

De Sosa, L.L., Glanville, H.C., Marshall, M.R., Schnepf, A., Cooper, D. M., Hill, P.W., Binley, A., Jones, D., 2018. Stoichiometric constraints on the microbial processing of carbon with soil depth along a riparian hillslope. Biology and Fertility of Soils 54, 949–963.

Denef, K., Zotarelli, L., Boddey, R.M., Six, J., 2007. Microaggregate associated C as a diagnostic fraction for management-induced changes in soil organic carbon in two Oxisols. Soil Biology & Biochemistry 39, 1165–1172.

Dormaar, J.F., 1992. Decomposition as a Process in Natural Grasslands. In: Couland, R.T., ed. Naturalgrasslands, Introduction and Western Hemisphere (ecosystems of the world). Amsterdam: Elsevier pp. 121–136.

Elliott, E.T., 1986. Aggregate structure and carbon, nitrogen, and phosphorus in native and cultivated soils. Soil Science Society of America Journal 50, 627–633.

Fischer, H., Ingwersen, J., Kuzyakov, Y., 2010. Microbial uptake oflow-molecular-weight organic substances out-competes sorption in soil. European Journal of Soil Science 61, 504–513.

Fischer, H., Kuzyakov, Y., 2010. Sorption, microbial uptake and decomposition of acetate in soil: transformations revealed by position-specific ^{14}C labelling. Soil Biology & Biochemistry 42, 186–192.

Ge, T., Li, B., Zhu, Z., Hu, Y., Yuan, H., Dorodnikov, M., Jones, D.L., Wu, J., Kuzyakov, Y., 2017. Rice rhizodeposition and its utilization by microbial groups depends on N fertilization. Biology and Fertility of Soils 53, 37–48.

Ge, T., Liu, C., Yuan, H., Zhao, Z., Wu, X., Zhu, Z., Brookes, P., Wu, J., 2015. Tracking the photosynthesized carbon input into soil organic carbon pools in a rice soil fertilized with nitrogen. Plant and Soil 392, 17–25.

Ge, T., Luo, Y., He, X., 2019. Quantitative and mechanistic insights into the key process in the rhizodeposited carbon stabilization, transformation and utilization of carbon, nitrogen and phosphorus in paddy soil. Plant and Soil 445, 1–5.

Ge, T., Wu, X., Chen, H., Yuan, H.Z., Li, B., Zhou, P., Liu, C., Tong, C., Brookes, P., Wu, J., 2013. Microbial phototrophic fixation of atmospheric CO_2 in China subtropical available upland and paddy soils. Geochimica et Cosmochimica Acta 113, 70–78.

Gregory, P.J., 2006. Roots, rhizosphere and soil: the route to a better understanding of soil science? European Journal of Soil Science 57, 2–12.

Hooker, B., Morris, T., Peters, R., Cardon, Z., 2005. Long-term effects of tillage and corn stalk return on soil carbon dynamics. Soil Science Society of America Journal 69, 188–196.

Jastrow, J.D., Amonette, J.E., Bailey, V.L., 2007. Mechanisms controlling soil carbon turnover and their potential application for enhancing carbon sequestration. Climatic Change 80, 5–23.

Johnson, J.M.F., Allmaras, R.R., Reicosky, D.C., 2006. Estimating source carbon from crop residues, roots and rhizodeposits using the National Grain-Yield Database. Agronomy Journal 98, 622–636.

Jones, D.L., Clode, P.L., Kilburn, M.R., Stockdale, E.A., Murphy, D.V., 2013. Competition between plant and bacterial cells at the microscale regulates the dynamics of nitrogen acquisition in wheat (*Triticum aestivum*). New Phytologist 200, 796–807.

Jones, D.L., Hodge, A., Kuzyakov, Y., 2004. Plant and mycorrhizal regulation of rhizodeposition. New Phytologist 163, 459–480.

Jones, D.L., Nguyen, C., Finlay, R.D., 2009. Carbon flow in the rhizosphere: carbon trading at the soil-root interface. Plant and Soil 321, 5–33.

Keiluweit, M., Bougoure, J.J., Nico, P.S., Pett-Ridge, J., Weber, P.K., Kleber, M., 2015. Mineral protection of soil carbon counteracted by root exudates. Nature Climate Change 5, 588–595.

Kong, A.Y., Six, J., Bryant, D.C., Denison, R.F., Van Kessel, C., 2005. The relationship between carbon input, aggregation, and soil organic carbon stabilization in sustainable cropping systems. Soil Science Society of America Journal 69, 1078–1085.

Kuzyakov, Y., 2002. Review: Factors affecting rhizosphere priming effects. Journal of Plant Nutrition and Soil Science 165, 382–396.

Kuzyakov, Y., 2010. Priming effects: interactions between living and dead organic matter. Soil Biology & Biochemistry 42, 1363–1371.

Kuzyakov, Y., Jones, D.L., 2006. Glucose uptake by maize roots and its transformation in the rhizosphere. Soil Biology & Biochemistry 38, 851–860.

Kuzyakov, Y., Larionova, A.A., 2005. Root and rhizomicrobial respiration: a review of approaches to estimate respiration by autotrophic and heterotrophic organisms in soil. Journal of Plant Nutrition and Soil Science 168, 503–520.

Leuschner, C., Gebel, S., Rose, L., 2013. Root trait responses of six temperate grassland species to intensive mowing and NPK fertilisation: a field study in a temperate grassland. Plant and Soil 373, 687–698.

Li, Q., Li, B.H., Kronzucker, H.J., Shi, W.M., 2010. Root growth inhibition by NH_4^+ in Arabidopsis is mediated by the root tip and is linked to NH_4^+ efflux and GMPase activity. Plant, Cell & Environment 33, 1529-1542 .

Li, Y., Li, Y., Chang, S.X., Liang, X., Qin, H., Chen, J., Xu, Q., 2017. Linking soil fungal community structure and function to soil organic carbon chemical composition in intensively managed subtropical bamboo forests. Soil Biology & Biochemistry 107, 19–31.

Linkohr, B.I., Williamson, L.C., Fitter, A.H., Leyser, H.M.O., 2002. Nitrate and phosphate availability and distribution have different effects on root system architecture of *Arabidopsis*. Plant Journal 29, 751–760.

Liu, Y., Ge, T., Ye, J., Liu, S., Shibistova, O., Wang, P., Wang, J., Li, Y., Guggenberger, G., Kuzyakov, Y., Wu, J., 2019a. Initial utilization of rhizodeposits with rice growth in paddy soils: Rhizosphere and N fertilization effects. Geoderma 338, 30–39.

Liu, Y., Ge, T., Zhu, Z., Liu, S., Luo, Y., Li, Y., Wang, P., Gavrichkova, O., Xu, X., Wang, J., Wu, J., Guggenberger, G., Kuzyakov, Y., 2019b. Carbon input and allocation by rice into paddy soils: A review. Soil Biology & Biochemistry 133, 97–107.

Lopez-Sangil, L., Rovira, P., 2013. Sequential chemical extractions of the mineral-associated soil organic matter: An integrated approach for the fractionation of organo-mineral complexes. Soil Biology &

Biochemistry 62, 57–67.

Lu, Y., Watanabe, A., Kimura, M., 2002. Contribution of plant- derived carbon to soil microbial biomass dynamics in a paddy rice microcosm. Biology and Fertility of Soils 36, 136–142.

Lu, Y., Watanabe, A., Kimura, M., 2003. Carbon dynamics of rhizodeposits, root- and shoot-residues in a rice soil. Soil Biology & Biochemistry 35, 1223–1230.

Luo, Y., Zhu, Z., Liu, S., Peng, P., Xu, J., Brookes, P., Ge, T., Wu, J., 2018. Nitrogen fertilization increases rice rhizodeposition and its stabilization in soil aggregates and the humus fraction. Plant and Soil 445, 1–11.

Mooshammer, M., Wanek, W., Zechmeister-Boltenstern, S., Richter, A., 2014. Stoichiometric imbalances between terrestrial decomposer communities and their resources: mechanisms and implications of microbial adaptations to their resources. Frontiers in Microbiology 5, 22.

Nguyen, C., 2009. Rhizodeposition of Organic C by Plant: Mechanisms and Controls. Dordrecht: Springer, pp. 97–123.

Norby, R.J., Cotrufo, M.F., Ineson, P., O'Neill, E.G., Canadell, J.G., 2001. Elevated CO_2, litter chemistry, and decomposition: a synthesis. Oecologia 127, 153–165.

Oades, J.M., 1988. The retention of organic matter in soils. Biogeochemistry 5, 35–70.

Pan, G., Li, L., Wu, L., Zhang, X., 2004. Storage and sequestration potential of topsoil organic carbon in China's paddy soils. Global Change Biology 10, 79–92.

Pan, G.X., Wu, L.S., Li, L.Q., Zhang, X.H., Gong, W., Wood, Y., 2008. Organic carbon stratification and size distribution of three typical paddy soils from Taihu Lake region China. Journal of Environmental Sciences (China) 20, 456–463.

Pausch, J., Tian, J., Riederer, M., Kuzyakov, Y., 2013. Estimation of rhizodeposition at field scale: upscaling of a ^{14}C labelling study. Plant and Soil 364, 273–285.

Pendall, E., Mosier, A.R., Morgan, J.A., 2004. Rhizodeposition stimulated by elevated CO_2 in a semi-arid grassland. New Phytologist 162, 447–458.

Pett-Ridge, J., Firestone, M.K., 2017. Using stable isotopes to explore root-microbe-mineral interactions in soil. Rhizosphere 3, 244–253.

Phillips, R.P., Finzi, A.C., Bernhardt, E.S., 2011. Enhanced root exudation induces microbial feedbacks to N cycling in a pine forest under long-term CO_2 fumigation. Ecology Letters 14, 187–194.

Recous, S., Robin, D., Darwis, D., Mary, B., 1995. Soil inorganic N availability: effect on maize residue decomposition. Soil Biology & Biochemistry 27, 1529–1538.

Rillig, M.C., Mummey, D.L., 2006. Mycorrhizas and soil structure. New Phytologist 171, 41–53.

Schmidt, M.W., Torn, M.S., Abiven, S., Dittmar, T., Guggenberger, G., Janssens, I.A., Kleber, M., Kogel-Knabner, I., Lehmann, J., Manning, D.A., Nannipieri, P., Rasse, D.P., Weiner, S., Trumbore, S.E., 2011. Persistence of soil organic matter as an ecosystem property. Nature 478, 49–56.

Six, J., Conant, R.T., Paul, E.A., Paustian, K., 2002. Stabilization mechanisms of soil organic matter: implications for C-saturation of soils. Plant and Soil 241, 155–176.

Smith, A.P., Marín-Spiotta, E., De Graaff, M.A., Balser, T.C., 2014. Microbial community structure varies across soil organic matter aggregate pools during tropical land cover change. Soil Biology & Biochemistry 77, 292–303.

Tarnawski, S., Aragno, M., 2006. The influence of elevated CO_2 on diversity, activity and biogeochemical function of rhizosphere and soil bacterial communities. In Nosberger, J., Long, S.P., Norby, R. J., Stitt, M., Hendrey, G.R., Blum, H., eds. Managed ecosystems and CO_2—Case Studies, Processes and Perspectives (Ecological studies series 187th ed.). Berlin: Springer, pp. 393–409

Traore, O., Groleau-Renaud, V., Plantureux, S., Tubeileh, A., Boeuf-Tremblay, V., 2000. Effect of root mucilage and modelled root exudates on soil structure. European Journal of Soil Science 51, 575–581.

von Lützow, M., Kögel-Knabner, I., Ekschmitt, K., Flessa, H., Guggenberger, G., Matzner, E., Marschner, B., 2007. SOM fractionation methods: relevance to functional pools and to stabilization mechanisms. Soil Biology & Biochemistry 39, 2183–2207.

Wei, X., Hu, Y., Peng, P., Zhu, Z., Atere, C.T., O'Donnell, A.G., Wu, J., Ge, T., 2017. Effect of P stoichiometry on the abundance of nitrogen-cycle genes in phosphorus-limited paddy soil. Biology and Fertility of Soils 53, 767–776.

Wei, X., Zhu, Z., Liu, Y., Luo, Y., Deng, Y., Xu, X., Liu, S., Richter, A., Guggenberger, G., Wu, J., Ge, T., 2020. C:N:P stoichiometry regulates soil organic carbon mineralization and concomitant shifts in microbial community composition in paddy soil. Biology and Fertility of Soils.

Wei, X., Zhu, Z., Wei, L., Wu, J., Ge, T., 2019. Biogeochemical cycles of key elements in the paddy-rice rhizosphere: microbial mechanisms and coupling processes. Rhizosphere 10, 100145.

Wu, J., Joergensen, R.G., Pommerening, B., Chaussod, R., Brookes, P.C., 1990. Measurement of soil microbial biomass C by fumigation-extraction—an automated procedure. Soil Biology & Biochemistry 22, 1167–1169.

Wu, J.S., 2011. Carbon accumulation in paddy ecosystems in subtropical China: evidence from landscape studies. European Journal of Soil Science 62, 29–34.

Wu, Y., Wu, J., Ma, Y., Lian, Y., Sun, H., Xie, D., Li, Y., Brookes, P., Yao, H., 2019. Dynamic changes in soil chemical properties and microbial community structure in response to different nitrogen fertilizers in an acidified celery soil. Soil Ecology Letters 1, 105–113.

Xiao, M., Zang, H., Liu, S., Ye, R., Zhu, Z., Su, Y., Wu, J., Ge, T., 2019. Nitrogen fertilization alters the distribution and fates of photosynthesized carbon in rice–soil systems: A ^{13}C–CO_2 pulse labeling study. Plant and Soil 445, 101–112.

Yang, Y.H., Luo, Y.Q., Lu, M., Schadel, C., Han, W.X., 2011. Terrestrial C:N stoichiometry in response to elevated CO_2 and N addition: a synthesis of two meta-analyses. Plant and Soil 343, 393–400.

Ye, R., Doane, T.A., Morris, J., Horwath, W.R., 2015. The effect of rice straw on the priming of soil organic matter and methane production in peat soils. Soil Biology & Biochemistry 81, 98–107.

Yuan, H., Zhu, Z., Liu, S., Ge, T., Jing, H., Li, B., Liu, Q., Lynn, T.M., Wu, J., Kuzyakov, Y., 2016. Microbial utilization of rice root exudates:^{13}C labeling and PLFA composition. Biology and Fertility of Soils 52, 615–627.

Zang, H., Blagodatskaya, E., Wang, J., Xu, X., Kuzyakov, Y., 2017.

Nitrogen fertilization increases rhizodeposit incorporation into microbial biomass and reduces soil organic matter losses. Biology and Fertility of Soils 53, 419–429.

Zang, H., Xiao, M., Wang, Y., Ling, N., Wu, J., Ge, T., Kuzyakov, Y., 2019. Allocation of assimilated carbon in paddies depending on rice age, chase period and N fertilization: Experiment with $^{13}CO_2$ labelling and literature synthesis. Plant and Soil 445, 113–123.

Zhao, Y., Shao, S., Schaeffer, S.M., Bao, X., Zhang, W., Zhu, B., He, H., Zhang, X., 2019. Methodological clarification for estimating the input of plant-derived carbon in soils under elevated CO_2 based on a ^{13}C-enriched CO_2 labeling experiment. Plant and Soil 440, 569–580.

Zhao, Z., Ge, T., Gunina, A., Li, Y., Zhu, Z., Peng, P., Wu, J., Kuzyakov, Y., 2018. Carbon and nitrogen availability in paddy soil affects rice photosynthate allocation, microbial community composition, and priming: combining continuous ^{13}C labeling with PLFA analysis. Plant and Soil 445, 137–152

Zhen, S., Zhou, J., Deng, X., Zhu, G., Cao, H., Wang, Z., Yan, Y., 2016. Metabolite profiling of the response to high-nitrogen fertilizer during grain development of bread wheat (*Triticum aestivum* L.). Journal of Cereal Science 69, 85–94.

Zhu, Z., Ge, T., Hu, Y., Zhou, P., Wang, T., Shibistova, O., Guggenberger, G., Su, Y., Wu, J., 2017. Fate of rice shoot and root residues, rhizodeposits, and microbial assimilated carbon in paddy soil-part 2: turnover and microbial utilization. Plant and Soil 416, 243–257.

Zhu, Z., Ge, T., Liu, S., Hu, Y., Ye, R., Xiao, M., Tong, C., Kuzyakov, Y., Wu, J., 2018. Rice rhizodeposits affect organic matter priming in paddy soil: the role of N fertilization and plant growth for enzyme activities, CO_2 and CH_4 emissions. Soil Biology & Biochemistry 116, 369–377.

Zhu, Z., Zeng, G., Ge, T., Hu, Y., Tong, C., Shibistova, O., He, X., Wang, J., Guggenberger, G., Wu, J., 2016. Fate of rice shoot and root residues, rhizodeposits, and microbe-assimilated carbon in paddy soil – part 1: decomposition and priming effect. Biogeosciences 13, 4481–4489.

Ziska, L.H., Weerakoon, W., Namuco, O.S., Pamplona, R., 1996. The influence of nitrogen on the elevated CO_2 response in field-grown rice. Functional Plant Biology 23, 45–52.

Zou, P., Fu, J., Cao, Z., Ye, J., Yu, Q., 2015. Aggregate dynamics and associated soil organic matter in topsoils of two 2,000-year paddy soil chronosequences. Journal of Soils and Sediments 15, 510–522.